

## Coordinates for Mapping the Distribution of Magnetically Trapped Particles

CARL E. McILWAIN

*Department of Physics and Astronomy  
State University of Iowa  
Iowa City, Iowa*

**Abstract.** Dipole representations of the earth's magnetic field have been found to have insufficient accuracy for the study of magnetically trapped particles. A coordinate system consisting of the magnitude of the magnetic field  $B$  and the integral invariant  $I$  has been found to organize adequately measurements made at different geographic locations. The present paper shows that a parameter  $L = f(B, I)$  can be defined that retains most of the desirable properties of  $I$  and that has the additional property of organizing measurements along lines of force. Since the parameter  $L$  is the analog of a physical distance in a dipole field (the equatorial radius of a magnetic shell), it is usually found to present fewer conceptual difficulties than the integral invariant  $I$ .

**Introduction.** Considerable difficulties were encountered in the early attempts to map the measured intensities of trapped particles. The difficulties were chiefly due to the high spatial gradients in the intensities. At low altitudes in the inner zone, for example, a change in the distance from the center of the earth of 3 per cent results in an intensity change of over a factor of 10. The shape of the earth's field deviates more than 3 per cent from any possible dipole representation, and therefore attempts to use a dipole model for a coordinate system can be expected to produce rather chaotic results.

The present paper describes a coordinate system that not only takes account of the non-dipole character of the field but can also be used to organize measurements along lines of force as is necessary for most theoretical studies.

**Adiabatic invariants.** The use of adiabatic invariants in describing the motion of a particle in a magnetic field has been discussed by *Northrup and Teller* [1960]. In the present paper, the integral (or longitudinal) invariant at a point in space  $A$  is defined as

$$I = \oint_A^{A'} (1 - B_i/B)^{1/2} ds$$

where  $ds$  is the differential path length along the line of force connecting the point  $A$  with its conjugate point  $A'$ ,  $B_i$  is the magnitude of the magnetic field along the line of force,  $B$  is the magnitude of the magnetic field at the point  $A$ ,

and where the integral is to be taken along the line of force between the conjugate points. Defined in this manner,  $I$  can be considered to be a scalar field that has a definite value at each point in space and does not require reference to the motion of trapped particles. If there is no electric field, this definition is equivalent to

$$I = P^{-1} \oint_A^{A'} P_{\parallel} ds$$

where  $P$  is the total momentum of a particle that mirrors at the point in space  $A$ , and where  $P_{\parallel}$  is the component of momentum along the line of force. If we assume that all three adiabatic invariants are conserved for a given particle, then the values of  $I$  are the same at every point in space at which a given particle mirrors. If the energy and mirror point distributions of a set of trapped particles in time equilibrium do not change importantly during the time the slowest particles drift once around the earth (for example, the high energy protons in the inner zone), then the directional intensity perpendicular to the line of force will be the same at all points in space having the same values of  $B$  and  $I$ .

**Magnetic shells.** The points in space that have the same value of  $B$  and  $I$  form a ring in each hemisphere. A particle mirroring at this  $B$  and  $I$  will remain upon the surface (or 'shell') described by the lines of force that connect these rings.

In general, two particles that initially mirror

at different values of  $B$  along a particular line of force will not drift in longitude to the same lines of force. This means that the shells described by the trajectories of the two particles do not coincide. It will be shown however, that in the earth's magnetic field, this effect is relatively small. One important consequence of this fact is that the omnidirectional intensity as well as the directional intensity is constant along the loci of constant  $B$  and  $I$ .

*Definition of the magnetic shell parameter  $L$ .* The fact that all particles that drift through a given line of force will remain on approximately the same shell throughout their motion leads immediately to the desirability of finding a method of labeling all points in space with a number that is unique for each shell.

Each locus of constant  $B$  and  $I$  is a line that lies on a fixed shell. Any parameter that is a function of only  $B$  and  $I$  will, therefore, have the correct longitude dependence. The problem of defining a magnetic shell parameter is thus reduced to finding a function  $f(B, I)$  that is constant along lines of force. Such a function could be found empirically by examining the functions  $I_i = g_i(B)$  along lines of force calculated with a representation of the earth's field. An empirical fit is not necessary, however, because the average of the functions  $g_i(B)$  around a shell is well represented by the function obtained for a dipole field.

The integral invariant in a dipole field at a magnetic latitude  $\lambda$  on a line of force having an equatorial radial distance of  $R_0$  is given by

$$I = 2R_0 \int_0^{\lambda} \left\{ 1 - \left[ \frac{(1 + 3Y_a^2)^{1/2}}{(1 + 3Y^2)} \right]^{1/2} \cdot \left[ \frac{(1 - Y^2)^3}{(1 - Y_a^2)} \right]^{1/2} \right\} (1 + 3Y_a^2)^{1/2} dY_a \quad (1)$$

or

$$I = R_0 h_1(\lambda) \quad (2)$$

where  $Y = \sin \lambda$ . Now in a dipole field

$$B = \frac{M}{R_0^3 \cos^6 \lambda} (1 + 3 \sin^2 \lambda)^{1/2} \quad (3)$$

where  $M$  is the dipole magnetic moment. By (3) we see that

$$R_0^3 B / M = h_2(\lambda) \quad (4)$$

Equations (2) and (4) give

$$\begin{aligned} I^3 B / M &= R_0^3 B / M h_1^3(\lambda) \\ &= R_0^3 B / M h_3(R_0^3 B / M) = h_4(R_0^3 B / M) \end{aligned}$$

or

$$R_0^3 B / M = F(I^3 B / M) \quad (5)$$

The magnetic shell parameter  $L$  is now defined for a point in the earth's magnetic field by the equation

$$L^3 B / M = F(I^3 B / M) \quad (6)$$

where  $I$  and  $B$  are to be calculated for the point with a representation of the earth's field,  $M$  is the dipole moment of the earth,<sup>1</sup> and  $F$  is the function in equation 5 which is calculated with a dipole field.

A set of values for the function  $F$  is given in Table 1. For accurate computation of  $L$ , the following method can be used:

Let

$$\ln \left( \frac{L^3 B}{M} - 1 \right) = \sum_{n=0}^{\infty} a_n X^n \quad (7)$$

where  $X = \ln(I^3 B / M)$ . Sets of the coefficients  $a_n$  for different ranges of  $X$  are given in Table

TABLE 1. Values for Function  $F$

$I^3 B / M$	$L^3 B / M$
$2.37529 \times 10^{-15}$	1.00002
$1.72697 \times 10^{-13}$	1.00016
$3.70298 \times 10^{-11}$	1.00045
$2.37086 \times 10^{-9}$	1.00180
$2.70390 \times 10^{-8}$	1.00406
$1.52215 \times 10^{-7}$	1.00722
$5.82114 \times 10^{-7}$	1.01131
$1.74352 \times 10^{-6}$	1.01632
$4.41257 \times 10^{-6}$	1.02228
$9.87364 \times 10^{-6}$	1.02919
$2.01130 \times 10^{-5}$	1.03707
$3.80506 \times 10^{-5}$	1.04596
$6.78113 \times 10^{-5}$	1.05585
$1.15049 \times 10^{-4}$	1.06680
$1.87314 \times 10^{-4}$	1.07881
$2.94482 \times 10^{-4}$	1.09194
$4.49250 \times 10^{-4}$	1.10620
$6.67702 \times 10^{-4}$	1.12165
$9.69961 \times 10^{-4}$	1.13832
$1.38095 \times 10^{-3}$	1.15626

<sup>1</sup> The value  $M = 8.06 \times 10^{25}$  gauss cm<sup>3</sup> = 0.311653 gauss  $R_e^3$  ( $R_e = 6371.2$  km) has been found to be satisfactory.

TABLE 1. Continued

$I^3 B/M$	$L^3 B/M$
$1.93121 \times 10^{-3}$	1.17553
$2.65795 \times 10^{-3}$	1.19618
$3.60595 \times 10^{-3}$	1.21827
$4.82943 \times 10^{-3}$	1.24187
$6.39281 \times 10^{-3}$	1.26706
$8.37277 \times 10^{-3}$	1.29392
$1.08602 \times 10^{-2}$	1.32252
$1.39624 \times 10^{-2}$	1.35298
$1.78056 \times 10^{-2}$	1.38538
$2.25380 \times 10^{-2}$	1.41985
$2.83332 \times 10^{-2}$	1.45650
$3.53938 \times 10^{-2}$	1.49547
$4.39567 \times 10^{-2}$	1.53691
$5.42973 \times 10^{-2}$	1.58097
$6.67358 \times 10^{-2}$	1.62782
$8.16455 \times 10^{-2}$	1.67767
$9.94598 \times 10^{-2}$	1.73070
$1.20681 \times 10^{-1}$	1.78716
$1.45893 \times 10^{-1}$	1.84729
$1.75772 \times 10^{-1}$	1.91135
$2.11103 \times 10^{-1}$	1.97966
$2.52798 \times 10^{-1}$	2.05255
$3.01912 \times 10^{-1}$	2.13036
$3.59672 \times 10^{-1}$	2.21352
$4.27504 \times 10^{-1}$	2.30245
$5.07058 \times 10^{-1}$	2.39766
$6.00263 \times 10^{-1}$	2.49967
$7.09352 \times 10^{-1}$	2.60911
$8.36934 \times 10^{-1}$	2.72664
$9.86054 \times 10^{-1}$	2.85300
1.16025	2.98905
1.36367	3.13571
1.60116	3.29403
1.87843	3.46520
2.20216	3.65056
2.58020	3.85161
3.02183	4.07005
3.53799	4.30783
4.14164	4.56716
4.84816	4.85057
5.67587	5.16095
6.64657	5.50164
7.78642	5.87648
9.12680	6.28994
$1.07055 \times 10$	6.74720
$1.25680 \times 10$	7.25432
$1.47699 \times 10$	7.81840
$1.73787 \times 10$	8.44781
$2.04766 \times 10$	9.15245
$2.41655 \times 10$	9.94413
$2.85705 \times 10$	$1.08369 \times 10$
$3.38471 \times 10$	$1.18478 \times 10$
$4.01899 \times 10$	$1.29973 \times 10$
$4.78427 \times 10$	$1.43104 \times 10$
$5.71146 \times 10$	$1.58179 \times 10$
$6.83985 \times 10$	$1.75576 \times 10$
$8.21991 \times 10$	$1.95767 \times 10$
$9.91695 \times 10$	$2.19347 \times 10$

TABLE 1. Continued

$I^3 B/M$	$L^3 B/M$
$1.20162 \times 10^3$	$2.47069 \times 10$
$1.46301 \times 10^3$	$2.79896 \times 10$
$1.79085 \times 10^3$	$3.19079 \times 10$
$2.20532 \times 10^3$	$3.66255 \times 10$
$2.45179 \times 10^3$	$3.93495 \times 10$
$2.73402 \times 10^3$	$4.23601 \times 10$
$3.05069 \times 10^3$	$4.56967 \times 10$
$3.41513 \times 10^3$	$4.94049 \times 10$
$3.82642 \times 10^3$	$5.35387 \times 10$
$4.30241 \times 10^3$	$5.81615 \times 10$
$4.84311 \times 10^3$	$6.33486 \times 10$
$5.47285 \times 10^3$	$6.91896 \times 10$
$6.19343 \times 10^3$	$7.57921 \times 10$
$7.03884 \times 10^3$	$8.32855 \times 10$
$8.01427 \times 10^3$	$9.18267 \times 10$
$9.16824 \times 10^3$	$1.01607 \times 10^3$
$1.05125 \times 10^3$	$1.12862 \times 10^3$
$1.21182 \times 10^3$	$1.25883 \times 10^3$
$1.40095 \times 10^3$	$1.41032 \times 10^3$
$1.62942 \times 10^3$	$1.58767 \times 10^3$
$1.90201 \times 10^3$	$1.79669 \times 10^3$
$2.23574 \times 10^3$	$2.04483 \times 10^3$
$2.64005 \times 10^3$	$2.34175 \times 10^3$
$3.14300 \times 10^3$	$2.70014 \times 10^3$
$3.76361 \times 10^3$	$3.13689 \times 10^3$
$4.55081 \times 10^3$	$3.67477 \times 10^3$
$5.54426 \times 10^3$	$4.34504 \times 10^3$
$6.83524 \times 10^3$	$5.19133 \times 10^3$
$8.51087 \times 10^3$	$6.27578 \times 10^3$
$1.07567 \times 10^4$	$7.68892 \times 10^3$
$1.37789 \times 10^4$	$9.56603 \times 10^3$
$1.79974 \times 10^4$	$1.21153 \times 10^3$
$2.39555 \times 10^4$	$1.56683 \times 10^3$
$3.27489 \times 10^4$	$2.07743 \times 10^3$
$4.60402 \times 10^4$	$2.83877 \times 10^3$
$6.73169 \times 10^4$	$4.02645 \times 10^3$
$1.02942 \times 10^5$	$5.98740 \times 10^3$
$1.67841 \times 10^5$	$9.47159 \times 10^3$
$2.96984 \times 10^5$	$1.63048 \times 10^4$
$5.95512 \times 10^5$	$3.17247 \times 10^4$
$1.44453 \times 10^6$	$7.49153 \times 10^4$
$5.00559 \times 10^6$	$2.51887 \times 10^5$
$1.47748 \times 10^7$	$7.32706 \times 10^5$
$4.09266 \times 10^7$	$2.00752 \times 10^6$
$1.91226 \times 10^8$	$9.28013 \times 10^6$
$6.50554 \times 10^8$	$3.12969 \times 10^7$
$5.20779 \times 10^9$	$2.50188 \times 10^8$

2. This method introduces an error in  $L$  of less than 0.3 per cent for  $-\infty < X < \infty$  and less than 0.03 per cent for  $X < 10$ .

*Significance of  $L$ .* In general,  $L$  should be regarded as a parameter that retains most of the useful properties of  $I$  exactly and that is also approximately constant along lines of force. To gain some feeling for the meaning of  $L$ , it is

TABLE 2. Coefficients  $a_n$  for Different Ranges of  $X$

	$X < -16$	$-16 < X < 0$	$0 < X < 8$	$8 < X < 21$	$X > 21$
$a_0$	0.294	0.62290	0.62291	1.0824	-3.04
$a_1$	0.330	0.43351	0.43416	0.20395	1.00
$a_2$	0	$1.4495 \times 10^{-2}$	$1.3680 \times 10^{-2}$	$5.4145 \times 10^{-2}$	0
$a_3$	0	$1.2154 \times 10^{-3}$	$1.4784 \times 10^{-3}$	$-9.3218 \times 10^{-4}$	0
$a_4$	0	$5.9474 \times 10^{-5}$	$1.2413 \times 10^{-5}$	$-5.6831 \times 10^{-5}$	0
$a_5$	0	$1.5367 \times 10^{-6}$	$-8.1278 \times 10^{-6}$	$2.7879 \times 10^{-6}$	0
$a_6$	0	$1.5843 \times 10^{-8}$	$1.4604 \times 10^{-7}$	$-3.4751 \times 10^{-8}$	0

useful to remember that, for a pure dipole field, a magnetic shell is labeled by an  $L$  equal to the shell's equatorial radius.

For most purposes,  $B$  and  $L$  should be used

as the principal spatial coordinates. For studies involving intuition, it is sometimes desirable to use a coordinate system having a closer resemblance to the actual physical geometry. One

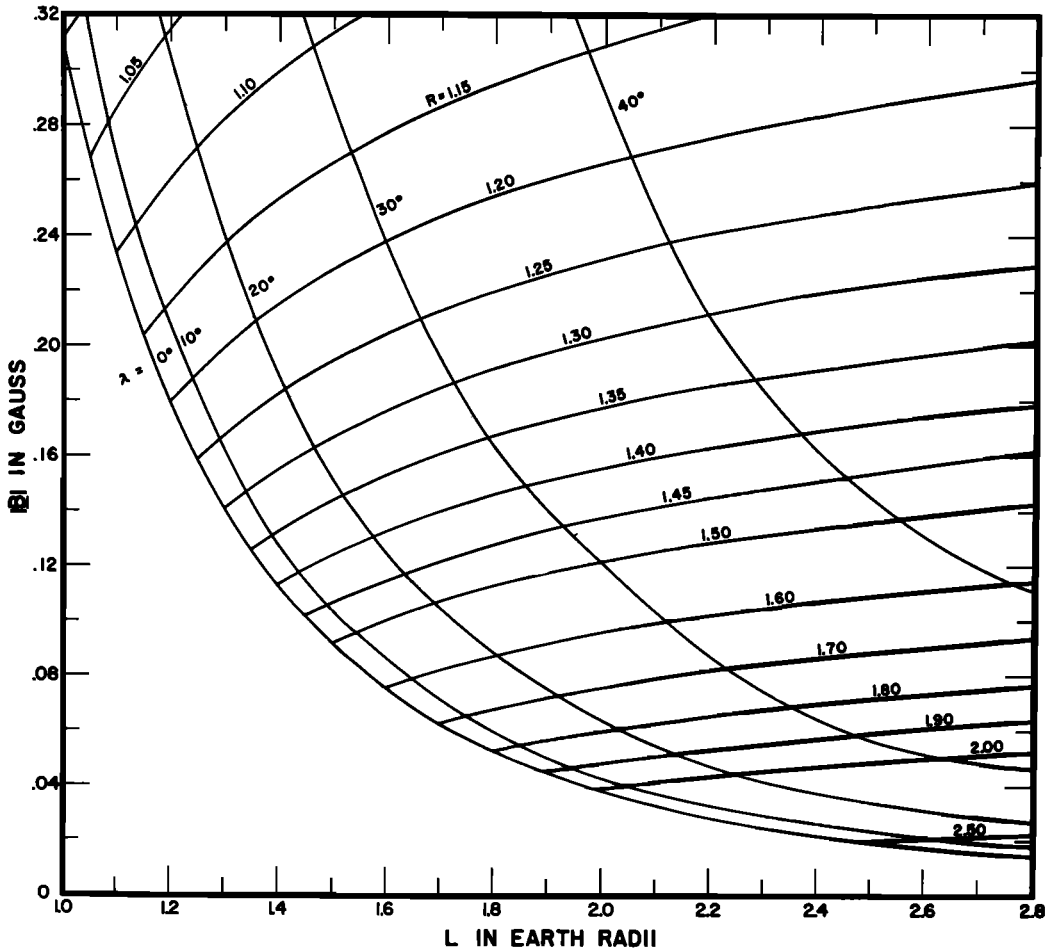


Fig. 1. The mapping of the polar coordinates  $R$  and  $\lambda$  on to the  $B, L$  plane according to the transformation

$$B = \frac{M}{R^3} \left( 4 - \frac{3R}{L} \right)^{1/2} \qquad R = L \cos^2 \lambda$$

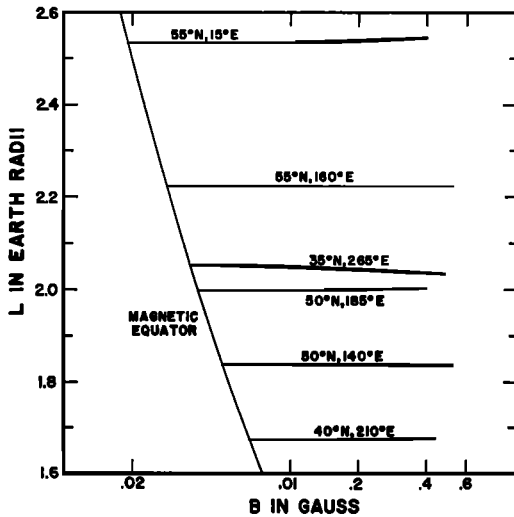


Fig. 2. The variation in  $L$  along six lines of force. Several of the worst cases are included.

system of this kind can be obtained by transforming  $B$  and  $L$  to polar coordinates using the dipole relations

$$B = \frac{M}{R^3} \left( 4 - \frac{3R}{L} \right)^{1/2}, \quad R = L \cos^2 \lambda \quad (8)$$

This relationship is illustrated in Figure 1.

A great deal of caution must be exercised when using the coordinates  $R$  and  $\lambda$  obtained in this manner, because although the irregular characteristics of the magnetic field will in effect be removed, geographic coordinates will transform in an irregular-longitude dependent manner.

*Variation of  $L$  along lines of force.* Tables of  $I$  versus  $B$  along 1400 different lines of force were kindly supplied to the author by D. C. Jensen, R. W. Murray, and J. A. Welch, Jr. These tables were computed with the 512 term

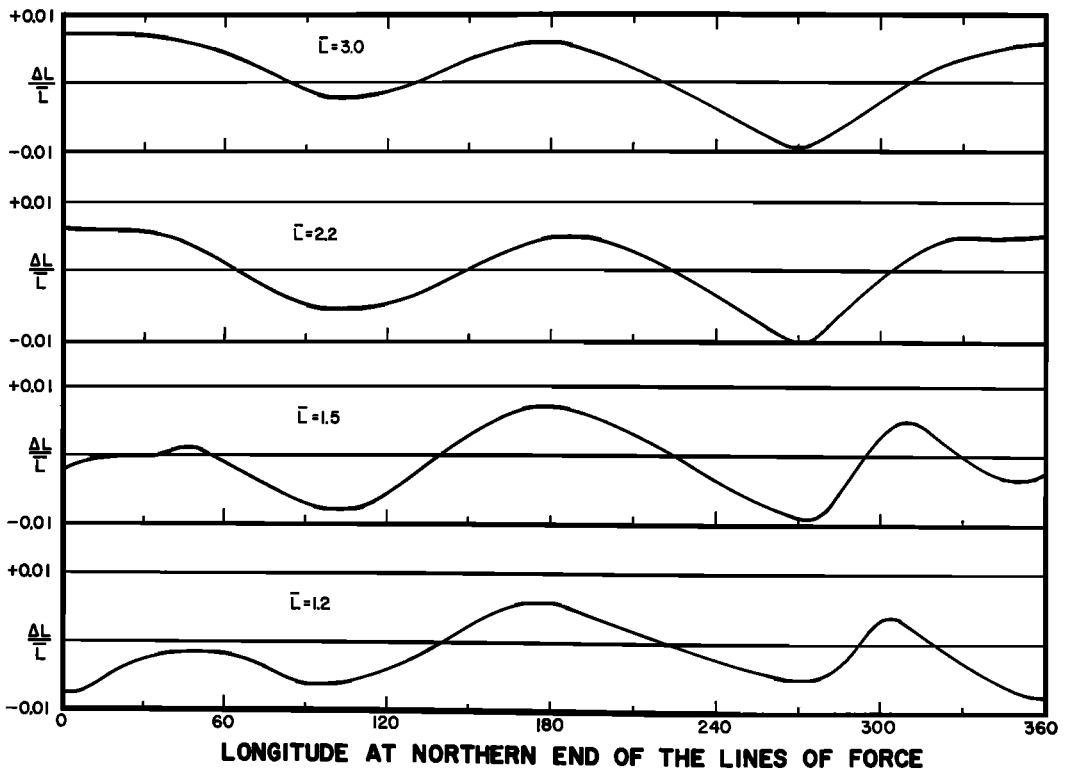


Fig. 3. The maximum deviation in  $L$  along lines forming magnetic shells labeled by  $L = 1.2, 1.5, 2.2$ , and  $3.0$  earth radii plotted versus the geographic longitude at the northern ends of the lines. A positive deviation means that  $L$  increased toward higher values of  $B$ .

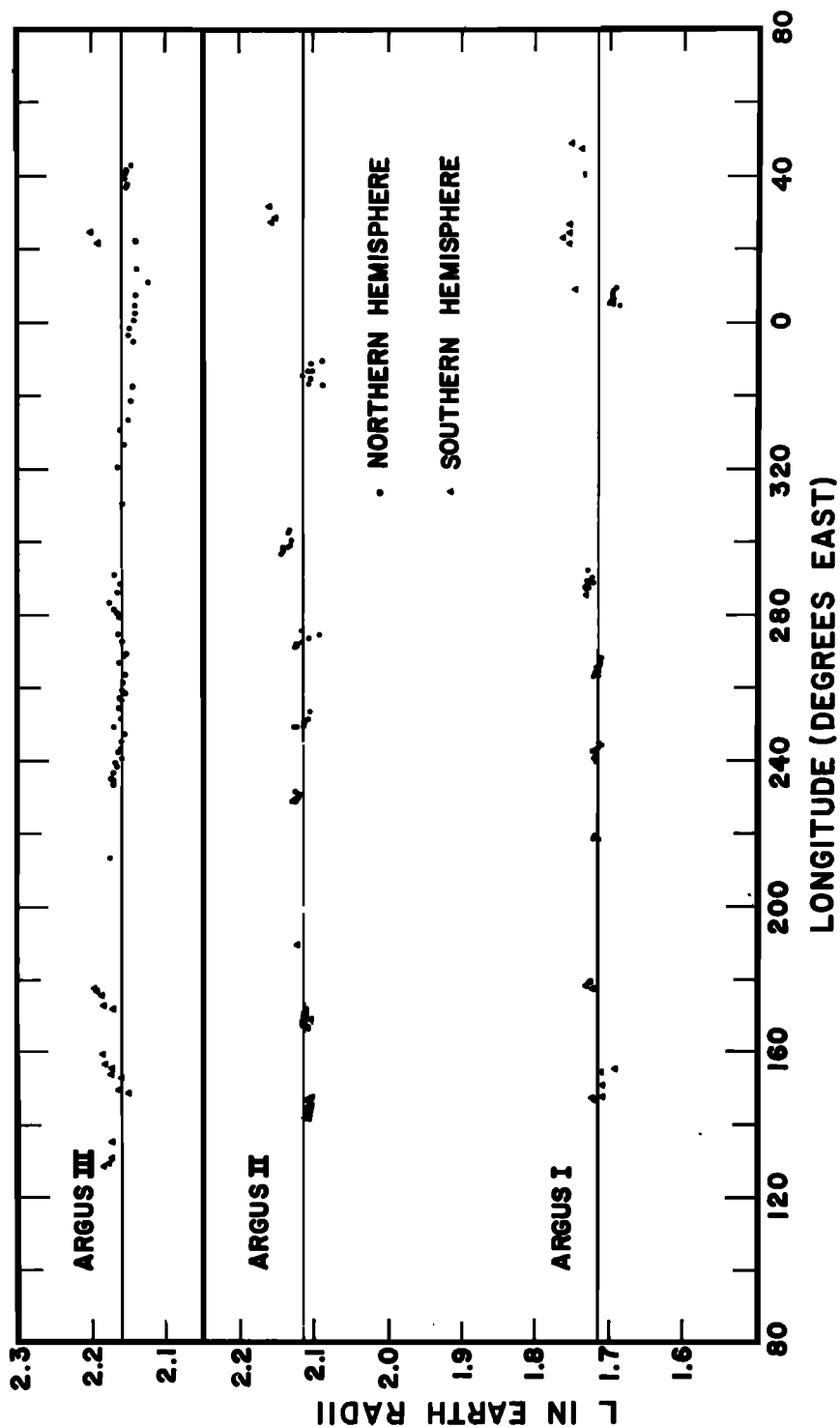


Fig. 4. The  $L$  values for the observed intersections of the Explorer IV trajectory with the three Argus shells are plotted versus geographic longitude.

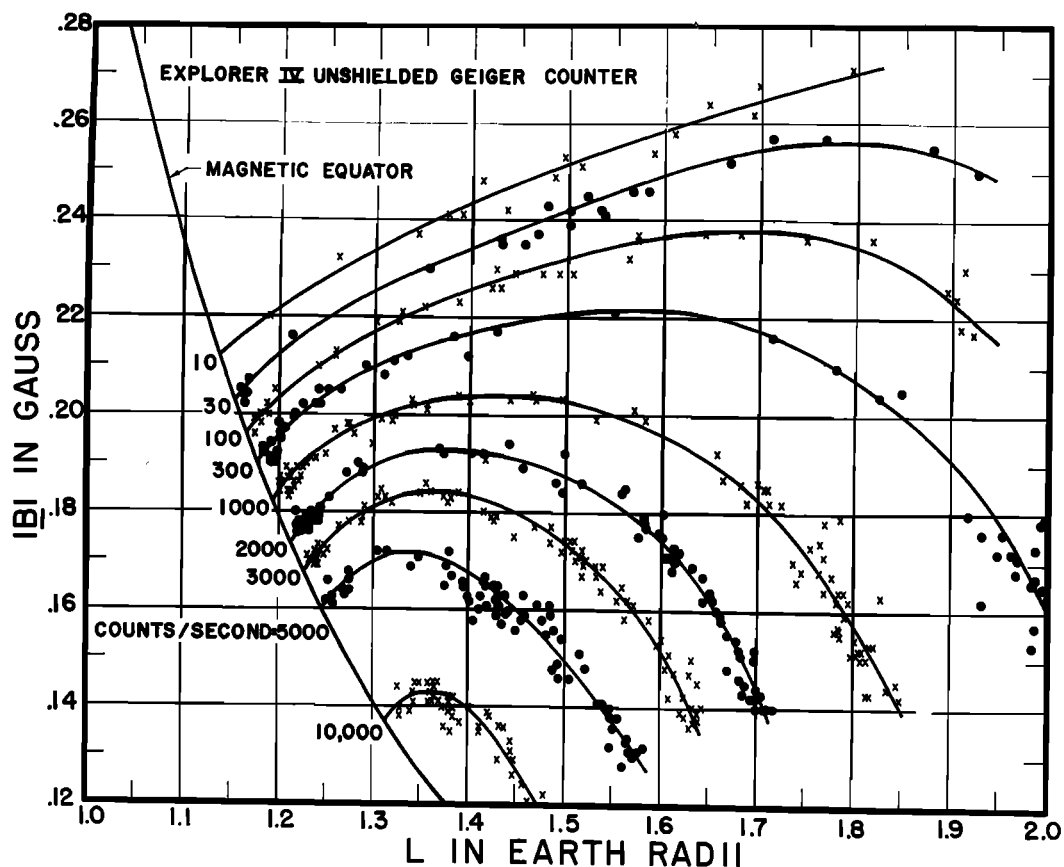


Fig. 5. Contours of constant true counting rate of the unshielded Geiger counter in Explorer IV. The points shown correspond to data obtained over a wide range of geographic latitude and longitude.

spherical harmonic expansion ( $n = 24, m = 17$ ) of the earth's field obtained by *Jensen and Whitaker* [1960] and from the 1955 surface data. The  $L$  values obtained from these sets of  $B$  and  $I$  were found to vary less than 1 per cent along most of the lines of force. Figure 2 shows the variation in  $L$  along six lines of force and includes several of the worst cases. The variations along different lines of force were found to be systematic in both latitude and longitude. This is illustrated in Figure 3 where the deviations in  $L$ , along lines forming the magnetic shells labeled by  $L = 1.2, 1.5, 2.2$ , and  $3.0$  earth radii, are plotted versus the geographic longitude at the northern ends of the lines. A positive deviation means that  $L$  increased toward higher values of  $B$ .

This kind of check upon the variation of  $L$  along lines of force tends to be independent of

the precision of the magnetic field analysis. An analysis of the earth's field based upon improved knowledge of the surface field would probably have nondipole terms of similar magnitude and therefore would be expected to give similar variations in  $L$  along lines of force. It should be noted, however, that, in the present analysis, the contributions of external current systems have been assumed to be zero.

*The Argus shells.* Well-defined shells of electrons injected by the three high altitude nuclear detonations Argus I, II, and III were detected by Satellite 1958 $\epsilon$  (Explorer IV) [*Van Allen, McIlwain, and Ludwig, 1959b*]. Each of the observed intersections of the satellite trajectory with an Argus shell should have the same value of  $L$ . Figure 4 shows the  $L$  values obtained for the observed intersections as a function of geographic longitude. The average  $L$  values for the

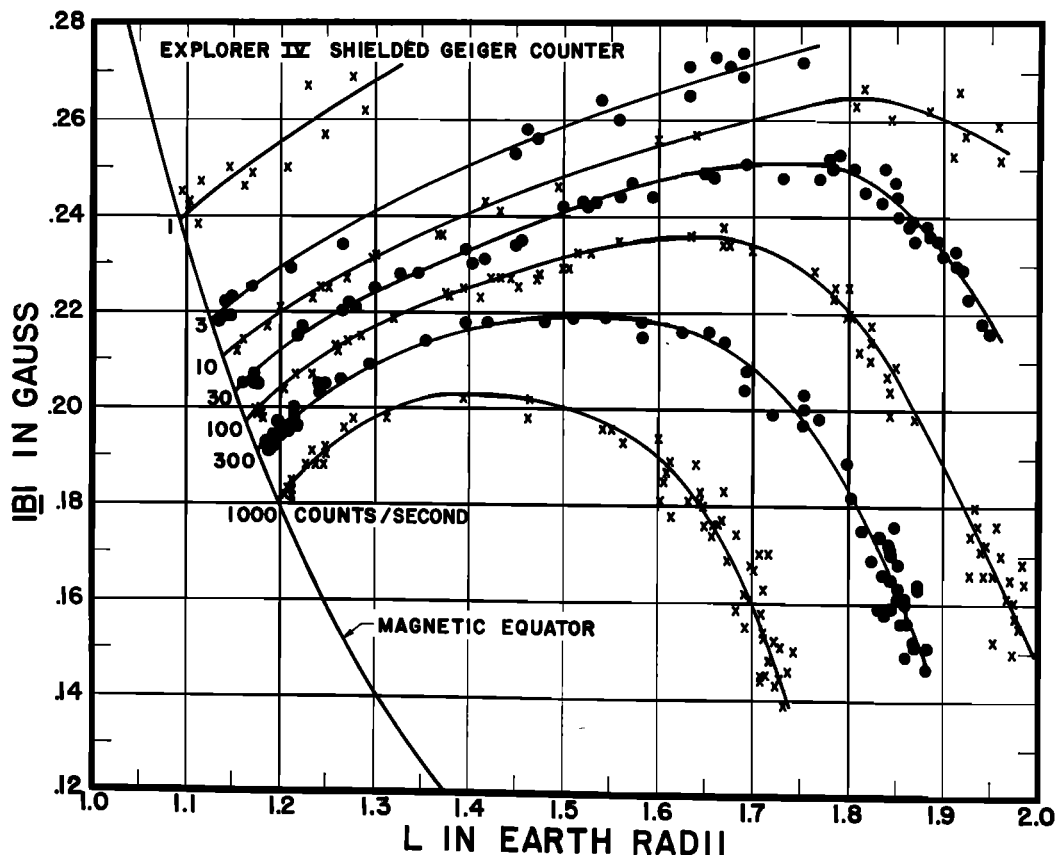


Fig. 6. Contours of constant true counting rate of the shielded Geiger counter in Explorer IV.

shells are 1.715, 2.115, and 2.16 earth radii for Argus I, II, and III, respectively. In addition to the scatter due to measurement inaccuracies, systematic variations with longitude of approximately  $\pm 1.5$  per cent can be discerned. By comparison, Pennington [1961] has found that the trace of the data points in the northern hemisphere for Argus III projected upon the surface of the earth deviates more than  $\pm 3.5^\circ$  from the earth trace of the best possible offset dipole shell. A latitude error of  $\pm 3.5^\circ$  for the Argus III shell corresponds to an error in  $L$  of about  $\pm 13$  per cent.

The range of  $B$  for the data points on each shell is not large. The deviations of the  $L$  values in Figure 4 are, therefore, almost entirely due to inaccuracies in the surface field upon which the magnetic field representation is based. It is interesting to note that the deviations in the  $L$  values are largest in the regions where the discrepancies between the various available maps

of the surface field are also large. No definite time dependence can be discerned in the data shown in Figure 4. An upper limit on the rate of change in  $L$  is 0.001 earth radii per day.

*Proton intensities in the inner zone.* The most complete set of data pertaining to the spatial distribution of particles in the inner zone presently available was obtained by the detectors on Satellite 1958e [Van Allen, McIlwain, and Ludwig, 1959a]. The results of a preliminary analysis of the Geiger tube data are shown in Figures 5 and 6. The geometric factors and proton thresholds are approximately  $0.54 \text{ cm}^2$  and 31 Mev for the unshielded counter and  $0.62 \text{ cm}^2$  and 43 Mev for the shielded counter. Comparison with the scintillation counter data indicates that most of the Geiger tube counting rates were probably due to penetrating protons rather than bremsstrahlung from the very much higher fluxes of nonpenetrating electrons.

The data points shown in Figures 5 and 6



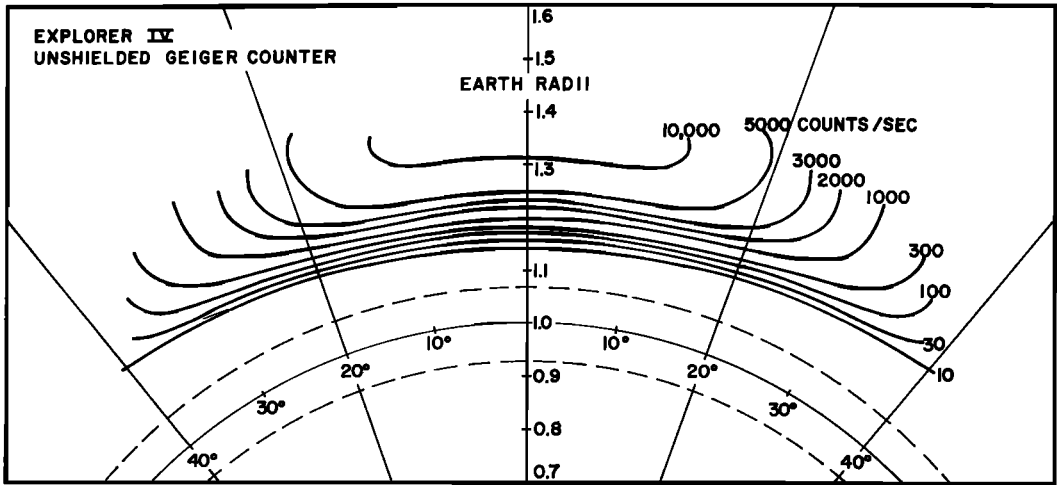


Fig. 7. The contours of constant counting rate shown in Figure 5 transformed to the polar coordinates  $R$  and  $\lambda$ .

were obtained from recordings made at stations in North and South America, Europe, Africa, Asia, Australia, New Zealand, and Hawaii. Data obtained during the periods immediately following high altitude nuclear detonations have been excluded.

The general physical configuration of the lower part of the inner zone is illustrated in Figures 7 and 8 where the  $B$  versus  $L$  curves in Figures 5 and 6 have been transformed into polar coordinates in the manner previously de-

scribed. The dashed lines approximately represent the maximum excursions of the earth's surface in these coordinates.

Some of the aspects of these graphs which will be subjects for future papers include: (a) determination of angular distributions in the manner outlined by Ray [1960]; (b) the spatial dependence of proton injection and loss mechanisms; (c) the spatial dependence of the proton energy spectrum; (d) the time dependence of the intensities; and (e) comparison with

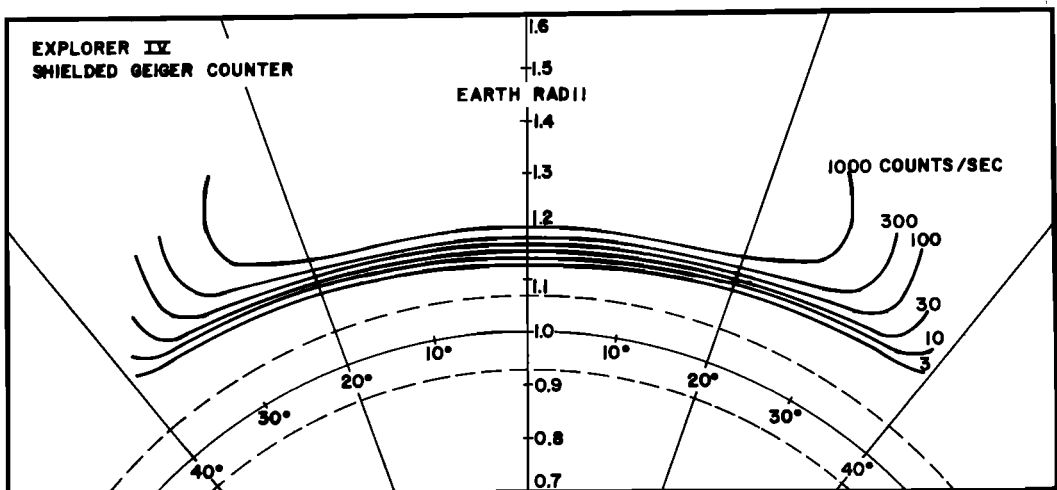


Fig. 8. The contours of constant counting rate shown in Figure 6 transformed to the polar coordinates  $R$  and  $\lambda$ .

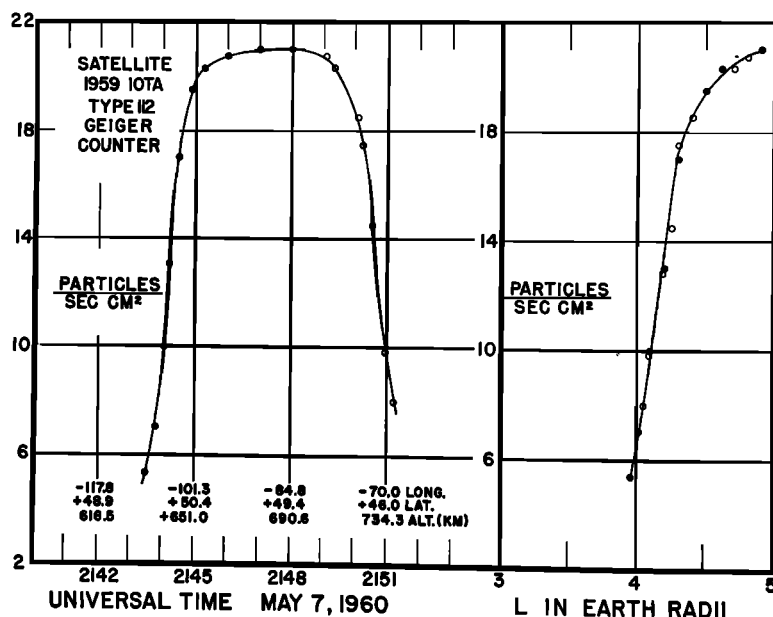


Fig. 9. The left side of this figure shows the omnidirectional intensity measured by the shielded Geiger counter aboard Explorer VII as a function of time during a solar cosmic ray event. The right side of the figure shows the same data points plotted versus  $L$ . On some occasions the modification of the earth's field by external current systems permits solar particles to arrive along lines of force labeled by considerably lower  $L$  values.

data obtained by instruments on other space vehicles.

*Solar cosmic rays.* The application of the  $B$  and  $L$  coordinate system is by no means limited to trapped particles; it can be usefully employed in the study of any phenomenon in which motion tends to be along lines of force. Some obvious examples are auroral particles, whistler mode wave propagation, and low energy cosmic rays.

The latitude dependence of solar cosmic rays is of particular interest in that it can be used to obtain information about both the energy spectrum of the particles and the distortion of the earth's magnetic field by external current systems. An example of the latitude dependence of solar cosmic rays is shown in Figure 9. The left side of this figure shows the intensity versus time measured by the shielded Geiger counter aboard Satellite 1959<sub>t</sub> (Explorer VII) during a solar cosmic ray event, and the right side shows the same data points plotted versus  $L$ .

*Time-varying magnetic field.* The magnetic shells labeled by  $L$  values greater than 3 earth radii are probably distorted by an important

amount during magnetic storms. It would be difficult if not impossible to calculate true instantaneous values of  $I$  during a magnetic storm. It is suggested that the values calculated for magnetically quiet periods be used as a fixed reference system in which the perturbations on the various phenomena can be studied.

*Computation of  $I$ .* Direct evaluation of  $I = \oint (1 - B_i/B)^{1/2} ds$  entails a considerable amount of computation. A number of relatively fast methods of computing  $I$  have been devised. At least one of these methods (which in general involve various means of interpolation) will probably be made available in the form of a computer program written in the Fortran language.

*Conclusion.* The choice of  $B$  and  $L$  as the primary coordinates is, of course, quite arbitrary. One possible alternate for  $B$  is  $B/B_0 = L^3 B/M$  where  $B_0 = M/L^3$  is the equatorial value of  $B$  on the line of force. It should be noted that any pair of the quantities  $B$ ,  $L$ ,  $R$ ,  $\lambda$ , and  $B/B_0$  can be used in place of  $B$  and  $L$ . To avoid confusion and to facilitate the comparison of different sets of data, it is suggested that a pair of

coordinates other than  $B$  and  $L$  be employed only if a substantially improved presentation is obtained.

*Acknowledgments.* I would like to thank Professor J. A. Van Allen and Professor E. C. Ray for their suggestions and helpful discussions. I would also like to thank Captain J. A. Welch, Jr., Mr. D. C. Jensen, and others at the Air Force Special Weapons Center for furnishing many of the necessary computations.

This research is supported in part by the Office of Naval Research (contract number Nonr 93803) and by the National Aeronautics and Space Administration (contract number NASw-17).

#### REFERENCES

- Jensen, D. C., and W. A. Whitaker, A spherical harmonic analysis of the geomagnetic field, *J. Geophys. Research*, **65**, 2500, 1960.
- Northrup, J. G., and E. Teller, Stability of the adiabatic motion of charged particles in the earth's magnetic field, *Phys. Rev.*, **117**, 215-225, 1960.
- Pennington, R. H., Equation of a charged particle shell in a perturbed dipole field, *J. Geophys. Research*, **66**, 709-712, 1961.
- Ray, E. C., On the theory of protons trapped in the earth's magnetic field, *J. Geophys. Research*, **65**, 1125-1134, 1960.
- Van Allen, J. A., C. E. McIlwain, and G. H. Ludwig, Radiation observations with satellite 1958e, *J. Geophys. Research*, **64**, 271-286, 1959a.
- Van Allen, J. A., C. E. McIlwain, and G. H. Ludwig, Satellite observations of electrons artificially injected into the geomagnetic field, *J. Geophys. Research*, **64**, 877-891, 1959b.

(Manuscript received August 28, 1961.)